Cancer Letters 561 (2023) 216139

Contents lists available at ScienceDirect

Cancer Letters

journal homepage: www.elsevier.com/locate/canlet

Local delivery of optimized nanobodies targeting the PD-1/PD-L1 axis with a self-amplifying RNA viral vector induces potent antitumor responses

Noelia Silva-Pilipich [a], Ester Blanco [a,b], Teresa Lozano [c], Eva Martisova [a], Ana Igea [a], Guillermo Herrador-Cañete [a], María Cristina Ballesteros-Briones [a], Marta Gorraiz [c], Patricia Sarrión [c], Gualberto González-Sapienza [d], Juan José Lasarte [c], Lucía Vanrell [e,f,**], Cristian Smerdou [a,*]

[a] Division of Gene Therapy and Regulation of Gene Expression, Cima Universidad de Navarra, Instituto de Investigación Sanitaria de Navarra (IdISNA), and CCUN, Pamplona, Spain
[b] Oncoimmunology Research Unit, Navarrabiomed-Universidad Pública de Navarra (UPNA), Instituto de Investigación Sanitaria de Navarra (IdiSNA), Pamplona, Spain
[c] Program of Immunology and Immunotherapy, Cima Universidad de Navarra, Instituto de Investigación Sanitaria de Navarra (IdISNA), and CCUN, Pamplona, Spain
[d] Cátedra de Inmunología, DEPBIO, Facultad de Química, Instituto de Higiene, UDELAR, Montevideo, Uruguay
[e] Facultad de Ingeniería, Universidad ORT Uruguay, Montevideo, Uruguay
[f] Nanogrow Biotech, Montevideo, Uruguay

ARTICLE INFO

Keywords:
Nanobody
SFV
Alphavirus
PD-1/PD-L1
Cancer immunotherapy

ABSTRACT

Despite the success of immune checkpoint blockade for cancer therapy, many patients do not respond adequately. We aimed to improve this therapy by optimizing both the antibodies and their delivery route, using small monodomain antibodies (nanobodies) delivered locally with a self-amplifying RNA (saRNA) vector based on Semliki Forest virus (SFV). We generated nanobodies against PD-1 and PD-L1 able to inhibit both human and mouse interactions. Incorporation of a dimerization domain reduced PD-1/PD-L1 IC50 by 8- and 40-fold for anti-PD-L1 and anti-PD-1 nanobodies, respectively. SFV viral particles expressing dimeric nanobodies showed a potent antitumor response in the MC38 model, resulting in >50% complete regressions, and showed better therapeutic efficacy compared to vectors expressing conventional antibodies. These effects were also observed in the B16 melanoma model. Although a short-term expression of nanobodies was observed due to the cytopathic nature of the saRNA vector, it was enough to generate a strong proinflammatory response in tumors, increasing infiltration of NK and $CD8^+$ T cells. Delivery of the SFV vector expressing dimeric nanobodies by local plasmid electroporation, which could be more easily translated to the clinic, also showed a potent antitumor effect.

1. Introduction

Tumor cells use many strategies to evade the immune system, such as engaging immune checkpoint (IC) pathways that induce immunosuppressive functions [1]. Among the different IC receptors, Cytotoxic T-Lymphocyte Antigen 4 (CTLA-4) and Programmed Death 1 (PD-1) are being used as therapeutic targets in different cancers [2]. Several monoclonal antibodies (mAbs) blocking these IC pathways (named IC inhibitors, or ICIs) have been shown to elicit a powerful antitumor effect that translates into significant and long-lasting clinical responses in a small fraction of patients [3,4]. So far, the FDA has approved seven different ICIs to treat more than 15 different types of cancer [5,6].

Nonetheless, most patients do not experience durable clinical benefits from these agents [5]. Furthermore, because these receptors constitute a natural mechanism to maintain self-tolerance, the systemic administration of ICIs results in an immune-based attack on normal tissues in a non-negligible fraction of patients [7]. These immune-related adverse events (irAEs) can potentially affect every organ of the body, being dermatitis and thyroiditis the most common ones, followed by others of major concern such as pneumonitis, colitis, hepatitis, hypophysitis, nephritis, myositis, and adrenalitis [8,9]. Therefore, there is an evident need to generate safer and more effective strategies to improve the treatment outcome in a higher percentage of patients.

* Corresponding author. Division of Gene Therapy and Regulation of Gene Expression, Cima Universidad de Navarra, Av. Pio XII 55, 31008, Pamplona, Spain.
** Corresponding author. Biotechnology laboratory, Facultad de Ingeniería, Universidad ORT Uruguay, Mercedes 1237, 11100, Montevideo, Uruguay.
E-mail addresses: lvanrell@nanogrowbiotech.com (L. Vanrell), csmerdou@unav.es (C. Smerdou).

https://doi.org/10.1016/j.canlet.2023.216139
Received 30 August 2022; Received in revised form 15 March 2023; Accepted 16 March 2023
Available online 29 March 2023

One strategy to limit irAEs could be to administer mAbs locally in tumors [10]. An attractive approach for local mAb delivery is the use of gene therapy vectors able to express mAbs inside the tumor mass [11,12], increasing antibody bioavailability and reducing systemic toxicity [13,14]. However, mAbs are large and complex molecules, which often leads to poor tissue penetration and low expression levels from gene therapy vectors. To overcome these drawbacks, the use of nanobodies (Nbs) instead of mAbs could be helpful.

Nbs (single-domain antibodies derived from the variable fragments of heavy-chain antibodies) are the smallest antigen-binding domains known so far in nature, with an approximate molecular mass of 15 kDa, and present several advantages related to their small size, single-domain nature and highly stable structure [15,16]. In the field of cancer therapy, some of their features are very attractive to design new therapeuticals: they can be easily engineered to dimerize, fuse to other domains that prolong their half-life or add new biological activities, without losing their high levels of expression from prokaryotic or eukaryotic cells [17,18]. Interestingly, Nbs have shown a very low immunogenicity in humans, as recently described in two clinical trials [19]. Because of their small size, even after being fused to other domains, they show high extravasation and tissue penetration [18]. However, their small size might also be a handicap, since they are rapidly eliminated from the bloodstream through renal clearance [20].

In the present study, we generated and characterized an original anti-Programmed Death Ligand 1 (PD-L1) Nb able to inhibit the interaction of PD-1 and PD-L1 for human and mouse molecules, and used a replication-defective alphavirus vector based on Semliki Forest virus (SFV) to deliver both anti-PD-1 (previously described by us [21]) and anti-PD-L1 Nbs. SFV-based RNA viral vectors have been developed for cancer vaccination and immunotherapy, and show several advantages over other vectors in preclinical models such as higher expression levels, broad tropism, induction of immunogenic apoptosis in tumor cells, and the ability to elicit powerful type I interferon (IFN–I) responses [22–24]. We reasoned that the SFV vector could not only enable a high and local intratumoral expression of the Nb but also elicit an important co-adjuvant response, which could synergize with the immunostimulatory and antitumoral activity of the Nb.

This study shows that, although monomeric Nbs conferred limited antitumor effect using this strategy, their modularity can be exploited to engineer molecules with stronger therapeutic potential. Fusion of Nbs to immunoglobulin G (IgG) fragment crystallizable (Fc) domains improved the PD-1/PD-L1 inhibition profile and promoted a more potent antitumor activity in a mouse model of colon adenocarcinoma compared to conventional antibodies. The feasibility of using SFV encoding a therapeutic Nb as a non-viral vector was also evaluated, which could simplify the manufacturing process and regulatory requirements for clinical translation.

2. Materials and methods

2.1. Cell lines and animals

BHK-21 cells (ATCC-CCL10) were cultured in GMEM-BHK21 (Thermo Fisher, Waltham, MA) supplemented with 5% fetal bovine serum (FBS), 10% tryptose phosphate broth, 2 mM glutamine, 20 mM HEPES and antibiotics (100 μg/mL streptomycin and 100 U/mL penicillin) (complete GMEM). HEK-293 (ATCC-CRL-3216) were cultured in DMEM (Gibco, BRL, UK) supplemented with 10% FBS, 2 mM glutamine and antibiotics. MC38 cells, a kind gift from Dr. Karl E. Hellström (University of Washington, Seattle, WA), were cultured in RPMI-1640 medium (Lonza, Switzerland) supplemented with 10% FBS, 2 mM glutamine, 20 mM HEPES, antibiotics and 50 μM 2-mercaptoethanol. B16-OVA and B16–F10 melanoma cells were kindly provided by Dr. Ignacio Melero (Cima Universidad de Navarra) and cultured in RPMI-1640 medium supplemented with 10% FBS, 2 mM glutamine, 20 mM HEPES, antibiotics, and 400 μg/mL of Geneticin for B16-OVA cells. Four or six-week-old female C57BL/6 mice were purchased from Envigo (Barcelona, Spain). Animal studies were approved by the Universidad de Navarra ethical committee (study number 078–19) for animal experimentation under Spanish regulations.

One adult female llama (*Lama glama*) from Montevideo municipal zoo (Uruguay) was used for immunization and construction of single-domain antibody library. The protocol was approved by the Parque Lecocq ethical committee (Montevideo) and manipulation of the llama was performed by veterinarians.

2.2. In vitro PD-1/PD-L1 inhibition assays

The ability of Nbs to inhibit the binding of PD-1 with PD-L1 was evaluated by competitive ELISAs. For human molecules, 96-well plates were coated with 100 μL/well of 0.5 μg/mL hPD-1-Fc (R&D, Minneapolis, MN) in PBS overnight (o/n) at 4 °C. After blocking with 300 μL/well of PBS-0.5% bovine serum albumin (BSA) for 1 h at room temperature (RT) and washing with PBS-0.05% Tween 20 (PBST), 100 μL of biotinylated hPD-L1 fused to human IgG Fc (BPS Bioscience, San Diego, CA) was added at 0.25 μg/mL, diluted in PBST-0.2% BSA, together with different concentrations of anti-PD-1 or anti-PD-L1 Nbs (or mAbs). Detection of hPD-L1 bound to hPD-1 was performed using streptavidin conjugated to peroxidase diluted in PBST-0.2% BSA for 1 h at RT, and the assay was developed using tetramethylbenzidine (TMB) substrate (BD Biosciences). For mouse molecules, a similar protocol was followed. In this case, 100 μL/well of 1 μg/mL mPD-L1-Fc (BioLegend, San Diego, CA) in PBS was used to coat the plates, and biotinylated mPD-1-Fc (BPS Bioscience) was used at 0.25 μg/mL. Commercial antibodies were included in these assays as controls of PD-1/PD-L1 inhibition: anti-mouse PD-1 (clone RMPI-14, BioXCell, Lebanon, NH), anti-mouse PD-L1 (clone 10F.9G2, BioXCell), nivolumab (Bristol Myers Squibb, New York, NY) and atezolizumab (Roche, Basel, Switzerland). The signal of wells incubated without Nbs or antibodies were considered 100% of PD-1/PD-L1 binding.

2.3. Production of recombinant SFV viral particles

SFV RNA was transcribed *in vitro* from SFV plasmids using SP6 RNA polymerase (Promega) and $m^7G(')ppp(5')G$ RNA Cap Structure Analog (New England Biolabs, Ipswich, MA). RNA synthesis and delivery into BHK-21 cells by electroporation was performed as described previously [25]. To produce SFV viral particles (VPs), two helper RNAs (SFV-helper-C-S219A and SFV-helper-S2) were co-electroporated together with the recombinant RNA, providing the SFV capsid and envelope proteins *in trans*, respectively [26]. Forty-eight hours after electroporation, supernatants were harvested, and VPs were purified by ultracentrifugation as described [27]. For titration of VPs, BHK-21 cells were infected with serial dilutions of the SFV vectors. For SFV-Nb11 and SFV-Nb6p, indirect immunofluorescence was performed using a mouse anti-HA primary antibody (BioLegend) and a secondary anti-mouse IgG antibody conjugated to Alexa-488 (Invitrogen, Waltham, MA). For antibodies with Fc domains, a direct immunofluorescence was performed using the same anti-mouse IgG antibody. SFV replicase (Rep) was detected with an in-house produced rabbit polyclonal antiserum that recognizes the nsp2 subunit. For SFV-LacZ, infected cells were treated with X-Gal staining solution and blue cells were counted as positive. Vector titers ranged from 2–6 x 10^{10} VPs/mL for SFV vectors coding for Nbs or antibodies, and 0.5–2 x 10^{11} VPs/mL for SFV-LacZ.

2.4. In vitro infection and transfection with SFV vectors for analysis of Nb expression

To analyze expression of Nbs *in vitro,* BHK-21 cells were infected with SFV VPs or transfected with pBK-T-SFV plasmids. After 24h, Nb expression was analyzed in cell extracts and supernatants by ELISA and Western blot as described in Supplemental Methods. For infection, 10^6

BHK-21 cells were seeded in six-well plates and after 24h they were infected with SFV VPs at a multiplicity of infection (MOI) of 20. VPs were diluted in 300 μL of MEM supplemented with 2 mM glutamine and 0.2% BSA and cells were infected for 1 h at 37 °C after which infection medium was replaced with complete GMEM. To evaluate expression of Nb11-Fc from pBK-T-SFV plasmid, 5×10^5 BHK-21 cells/well in 6-well plates were transfected with 2 μg of plasmid/well using lipofectamine-2000 (Thermo Fisher).

Supernatants and cell extracts from infected or transfected cells were collected after 24 h to evaluate antibody expression. Supernatants were centrifuged at 10,000 g for 5 min at 4 °C to eliminate cell debris. Cells were washed three times with PBS before incubating them with cold lysis buffer (50 mM Tris-HCl pH 7.5, 1% NP-40, 150 mM NaCl, 2 mM EDTA, and Protease Inhibitor Cocktail, Roche) for 10 min at 4 °C. Lysed cells were centrifuged at 6000 g for 10 min at 4 °C, and supernatants (containing proteins from lysed cells) were collected for analysis. Samples were stored at −80 °C until use.

2.5. Tumor induction and treatment with SFV viral vectors

Four-week-old female C57BL/6J mice were subcutaneously (s.c.) injected in the right flank with 5×10^5 tumor cells diluted in saline solution. Seven-ten days after tumor inoculation, SFV vectors were administered intratumorally (i.t.) in a total volume of 50 μL, diluted in saline solution. One dose of 3×10^8 VPs/tumor was used in all the experiments, unless otherwise specified. Control untreated mice received the same volume of saline solution.

The efficacy of treatments was evaluated by measuring two perpendicular tumor diameters every 2–3 days, and tumor volumes were calculated using the formula: volume = (Length x Width^2)/2. Mice were treated when the average tumor volume was approximately 30 mm^3 (MC38), 50 mm^3 (B16-OVA), or 80 mm^3 (B16–F10), and humanely sacrificed when tumor size reached ~1200 mm^3, or when tumor ulceration or evident discomfort were observed. For the bilateral tumor experiment, 5×10^5 and 3×10^5 MC38 cells were inoculated in the right and left flanks, respectively. The largest tumor was treated with two doses of SFV-Nb11-Fc administered 5 days apart (3×10^8 VPs/dose).

For rechallenge experiments in the MC38 model, mice that rejected tumors were injected s.c. with 5×10^5 MC38 cells in the left flank three months after the first tumor inoculation. Naïve mice were included as controls and development of tumors was evaluated for two months.

2.6. Non-viral delivery of SFV by electroporation

Six-week-old female C57BL/6J mice were challenged with 5×10^5 MC38 cells s.c. in the right flank. After ten days, intratumoral delivery of pBK-T-SFV plasmids harboring SFV replicons containing Nb11-Fc or LacZ genes was performed by electroporation as described previously [28]. Briefly, 2 h before treatment, hyaluronidase type IV (Sigma) was injected i.t. (30 units/tumor). 20 μg of pBK-T-SFV endotoxin-free plasmid/dose was used, diluted in 25 μL of PBS. Mice were anesthetized, plasmid was injected i.t. and, immediately after that, local electroporation was performed using the ECM 830 electroporation system (BTX, Holliston, MA) and the following conditions: eight pulses of 1200 V/cm of 0.1 ms duration each, with a 5 ms gap between pulses. This procedure was performed three times every three days. For the first round of treatment, tumors were exposed performing a simple surgery.

2.7. Statistical analysis

Data are expressed as the mean ± SD or mean ± SEM, as specified in each figure legend. Prism software (GraphPad Software, San Diego, CA) was used for statistical analysis. To compare multiple experimental groups, one-way ANOVA test and Tukey's multiple comparison test were used. Unpaired *t*-test was applied to compare two experimental groups. For time-series analysis, data were compared using the extra sum-of-squares F test and fitted to a second-order polynomial equation. Survival of tumor-bearing mice is represented by Kaplan–Meier plots and analyzed by log-rank test. The p values < 0.05 were considered statistically significant.

3. Results

3.1. Isolation and characterization of a new PD-L1-specific Nb

We have recently described the isolation of an anti-PD-1 Nb (Nb11) able to block PD-1/PD-L1 interactions for both human and mouse molecules [21]. In the present work we have developed a new Nb against PD-L1 from a llama immunized with human PD-L1 ectodomain, as described in supplemental methods. Briefly, we obtained cDNA from peripheral blood lymphocytes and generated a Nb library in phages, which allowed us to select specific clones by phage display (Supplemental Fig. 1A). After three rounds of selection, we obtained 21 clones able to bind to human PD-L1 as observed by flow-cytometry (Supplemental Fig. 1B) and ELISA assays (Supplemental Fig. 1C). By sequencing these clones, we identified nine different Nb sequences, which were cloned into a plasmid for *E. coli* expression and purified as described in supplemental methods. To evaluate whether the selected clones were able to inhibit binding of PD-L1 to PD-1, we performed an inhibition ELISA using commercially available PD-1 and PD-L1 ectodomains fused to human IgG1 Fc domain. All tested Nbs were able to inhibit binding of human PD-1 to PD-L1 (Supplemental Figs. 1D and E). We also evaluated the ability of these Nbs to inhibit the binding of murine domains in a similar inhibition ELISA and found two candidates able to inhibit PD-1/PD-L1 binding by more than 50% at 300 nM (Supplemental Fig. 1F). Of these two clones, Nb6p showed a markedly superior inhibition capacity, comparable to an anti-mouse PD-L1 antibody that had shown potent antitumor activity in a previous work (Supplemental Fig. 1G) [11]. Due to the cross-reactivity of Nb6p for human and murine molecules, this Nb was selected for further experiments.

3.2. Evaluation of SFV vectors encoding monomeric Nbs against PD-1 and PD-L1

We developed SFV vectors expressing both Nb11 and Nb6p in order to test their antitumor potential by local delivery to tumors. For that purpose, we cloned the Nb11 and Nb6p sequences into SFV, generating SFV-Nb11 and SFV-Nb6p vectors, respectively. In both cases the Nb sequence was designed with a signal peptide at the amino terminus, to allow secretion, and a hemagglutinin tag at the carboxyl terminus for detection (Fig. 1A). Nb expression was evaluated in BHK-21 cells infected with SFV-Nb11 and SFV-Nb6p VPs at 24h post-infection, and SFV-LacZ vector was used as control. Immunofluorescence (IF) analysis of infected cells showed co-expression of both Nb and SFV replicase (Rep) (Fig. 1B). Western blot analysis showed that both Nbs were expressed with the expected size (around 15 kDa) in cell extracts but showed a higher molecular weight (MW) in supernatants (Fig. 1C). This is in line with previous observations for Nb11 expressed from an AAV vector plasmid, in which we demonstrated that this shift was due to glycosylation and that it did not affect antigen binding [21]. Quantification of Nbs was performed by a specific ELISA against PD-1 or PD-L1, and in both cases we confirmed that the secretion was very effective, as the majority of the Nb (~85%) was present in supernatants. Expression levels were around 20 and 10 μg of secreted Nb11 and Nb6p, respectively, per 10^6 infected cells (Fig. 1D).

We then evaluated the antitumor activity of SFV-Nb11 and SFV-Nb6p vectors in a colon adenocarcinoma mouse model using MC38 cells implanted subcutaneously. Tumors were treated with 3×10^8 VPs intratumorally, a dose that had previously shown a significant antitumor effect in this model using a SFV vector encoding a full-length anti-PD-L1 mAb (SFV-aPDL1) [11]. However, despite the PD-1/PD-L1 blocking activity observed *in vitro* with Nb11 and Nb6p, only a modest antitumor

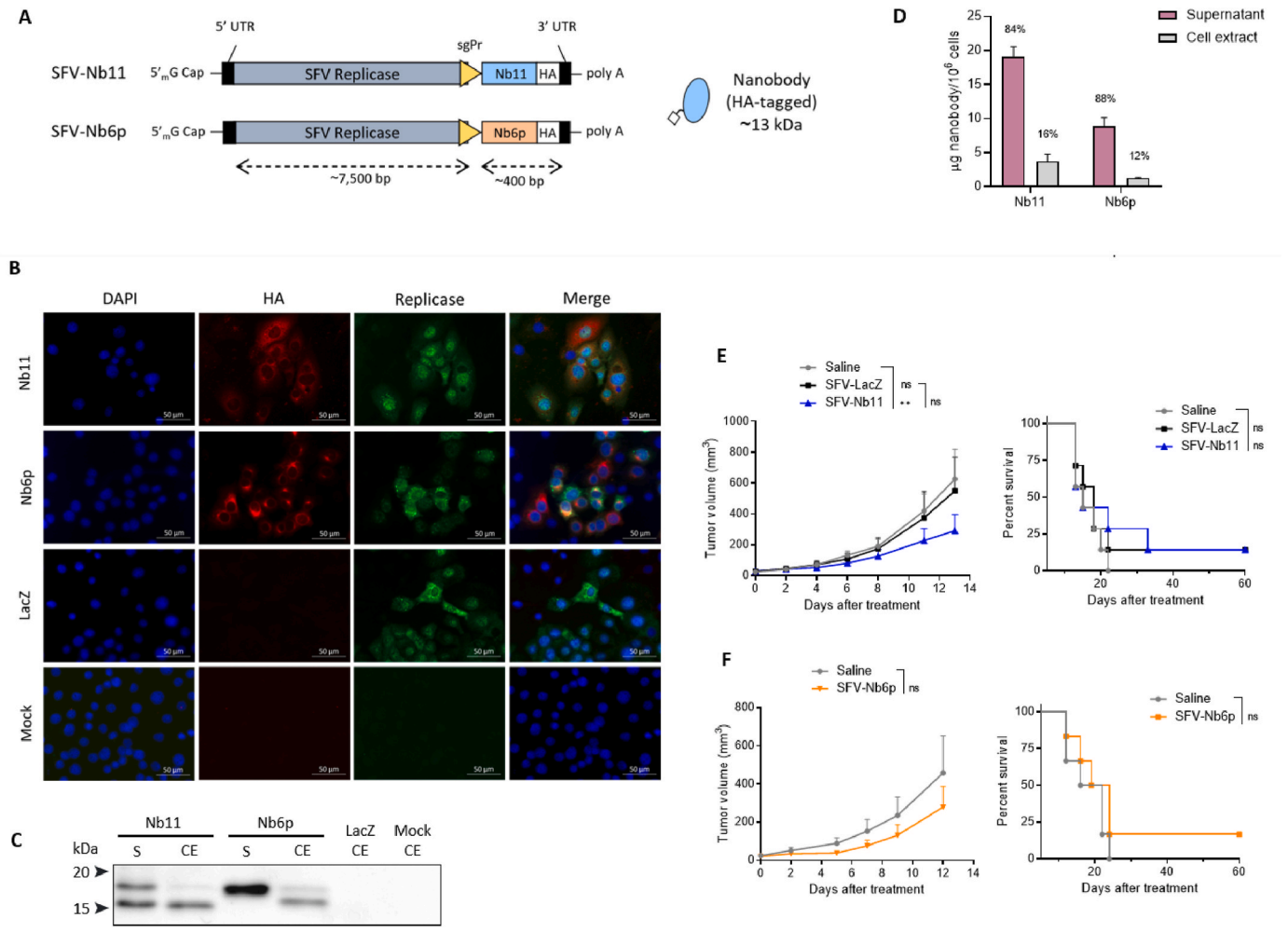

Fig. 1. Expression of anti-PD-1 and anti-PD-L1 Nbs from SFV vectors *in vitro* and evaluation of their antitumor activity. (**A**) Diagram of SFV vectors encoding monomeric Nbs, showingthe protein product on the right (not to scale). The subgenomic promoter (sgPr) that allows the transcription of the subgenomic RNA encoding the Nb is shown in yellow. (**B-D**) BHK-21 cells were infected with SFV VPs expressing the indicated transgenes using a MOI of 20, or mock infected, and analyzed at 24h by immunofluorescence using antibodies against HA tag and SFV replicase (**B**), Western blot, using anti-HA antibody (**C**), and specific PD-1 or PD-L1 binding ELISA for quantification (the percent of each fraction is indicated above bars) (**D**). (**E** and **F**) The antitumor activity of SFV vectors encoding monomeric anti-PD-1 (SFV–Nb11) (**E**) and anti-PD-L1 (SFV–Nb6p) (**F**) Nbs was evaluated in the MC38 subcutaneous tumor model using SFV-LacZ and saline as controls. Mice bearing ~30 mm^3 MC38 tumors received one intratumoral dose of 3×10^8 VPs. Left graphs, tumor growth after treatment. Data represent mean ± SEM (n = 6-7 per group), a representative experiment out of two with similar results is shown. Right graphs, survival curves of treated animals. UTR, untranslated region; HA, hemagglutinin tag; S, supernatant; CE, cell extract; ns, not significant; **, $p < 0.01$. Magnification in B, 400×.

effect was achieved using SFV-Nb11 and SFV-Nb6p vectors *in vivo*. A slight delay in the rate of tumor growth was observed, but without a significant improvement in survival (Fig. 1E and F). We hypothesized that the short half-life of Nbs [20] and the short-term expression provided by the SFV vector could be the reasons behind the low therapeutic efficacy of monomeric Nbs in these experimental settings.

3.3. Generation of SFV vectors encoding dimeric Nbs

Given the low antitumor activity observed with SFV vectors expressing Nb11 and Nb6p, we proceeded to modify these vectors by fusing each Nb sequence to an IgG Fc domain to promote their dimerization. The use of Nb dimers is usually more effective than the use of monomers [29], and fusion to IgG Fc domains has shown to provide a significant increase in the serum half-life of these molecules [30], suggesting that this modification could improve the performance of our vectors. For this purpose, Nb11 was fused to mouse IgG1 Fc domain (generating SFV-Nb11-Fc), an isotype with no secondary functions as PD-1 is expressed mainly on T cells (Fig. 2A). Nb6p was fused to mouse IgG2a Fc domain, generating SFV-Nb6p-Fc (Fig. 2A). This last isotype elicits strong antibody-dependent cellular cytotoxicity (ADCC) and complement-dependent cytotoxicity (CDC), which could be advantageous since PD-L1 is expressed on many tumor cells [31].

Expression of the Nb-Fc fusion molecules was first analyzed in BHK-21 cells infected with SFV-Nb11-Fc and SFV-Nb6p-Fc vectors. In this experiment we used as controls SFV vectors expressing conventional mAbs against murine PD-1 and PD-L1 (SFV-aPD1 and SFV-aPDL1 [11], respectively). As observed before, infected cells showed co-expression of both Nb-Fc and SFV Rep by IF (Fig. 2B). Quantification of antibodies from infected cells was performed by ELISA, observing a significantly higher expression of Nb-Fc molecules compared to mAbs (Fig. 2C). Nevertheless, the expression levels of dimeric Nbs were two to four-fold lower than those observed for the monomeric versions (Fig. 1D), although they were also efficiently secreted (Fig. 2C). Both Nb11-Fc and Nb6p-Fc were able to dimerize when analyzed by Western blot using non-reducing conditions (Fig. 2D, lower panel). Under reducing conditions, both Nb-Fc molecules showed the expected size (approximately 40 kDa, Fig. 2D, upper panel).

The fusion of Fc domains to Nb could have an impact on their antigen-binding properties, as dimerization could increase their avidity.

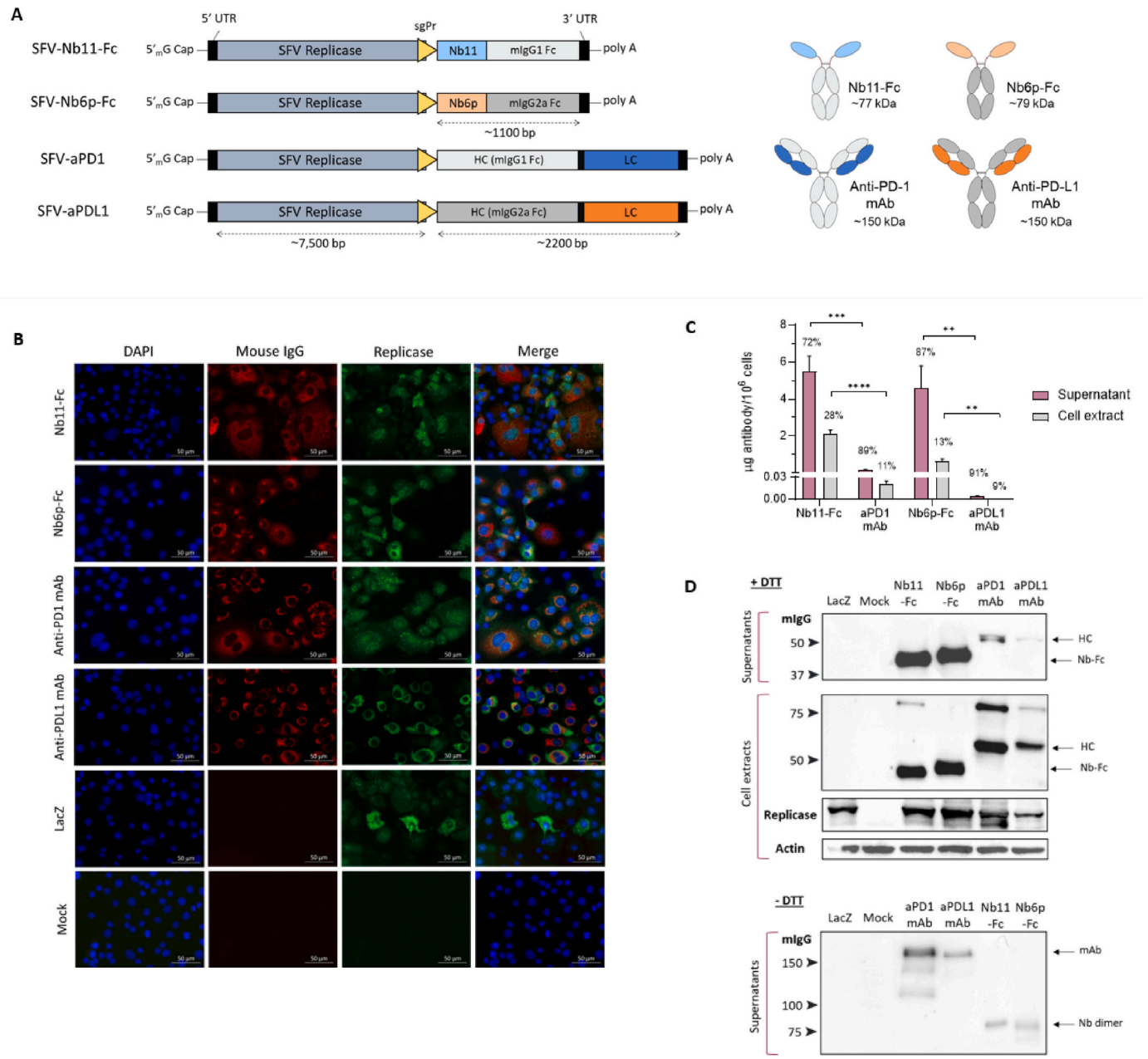

Fig. 2. Expression of Nb-Fc fusion proteins from SFV vectors *in vitro* compared to conventional antibodies. (**A**) Schematic diagrams of SFV vectors encoding Nbs against PD-1 and PD-L1 fused to the indicated mouse IgG (mIgG) Fc domains (SFV–Nb11-Fc and SFV-Nb6p-Fc, respectively), and conventional full-length antibodies (mAb) against mouse PD-1 and PD-L1 (SFV-aPD1 and SFV-aPDL1, respectively). On the right, schematic diagrams of the different antibodies and their estimated molecular weights are shown. (**B**–**D**) BHK-21 were infected with SFV VPs expressing the indicated transgenes using a MOI of 20, or mock infected, and analyzed at 24h by immunofluorescence using antibodies against mIgG and SFV replicase (**B**), specific IgG ELISA for quantification (the percent of each fraction is indicated above bars) (**C**), and Western blot using antibodies against mIgG, SFV replicase, and α-actin (**D**). UTR, untranslated region; sgPr, subgenomic promoter; DTT, dithiothreitol; HC, IgG heavy chain; LC, IgG light chain. Magnification in B, 400×.

To test whether this was the case, inhibition curves for PD-1/PD-L1 binding were compared using monomeric Nbs or the Fc-fused versions, which were previously purified from SFV-transfected cells as described in supplemental methods. Interestingly, fusion to Fc domains improved the inhibition potential of Nbs for mouse and human molecules with an approximate 40- and 8-fold IC50 reduction for Nb11-Fc and Nb6p-Fc, respectively (Fig. 3). We also included commercially available mAbs in these assays and observed that Nb6p-Fc had similar IC50 compared to both atezolizumab and clone 10F-9G2, an anti-mouse PD-L1 mAb commonly used in preclinical studies [32]. In the case of Nb11-Fc, we observed a 10- and 700-fold IC50 reduction when compared with nivolumab and clone RMPI-14, respectively. This last clone is an anti-mouse PD-1 mAb which has shown potent antitumor activity in preclinical studies [32,33].

3.4. Antitumor activity of SFV vectors encoding Nb-Fc

Since Nb-Fc fusions led to a decrease in the IC50 values for PD-1/PD-L1 inhibition, we reasoned that these molecules could have a better performance than monomeric Nbs *in vivo*. SFV vectors encoding Nb11-Fc and Nb6p-Fc were evaluated in the MC38 subcutaneous tumor model, including vectors encoding monomeric Nbs (SFV–Nb11 and SFV-Nb6p) and conventional mAbs (SFV-aPD1 and SFV-aPDL1) for comparison. SFV-Nb11-Fc and SFV-Nb6p-Fc showed a very potent antitumor effect,

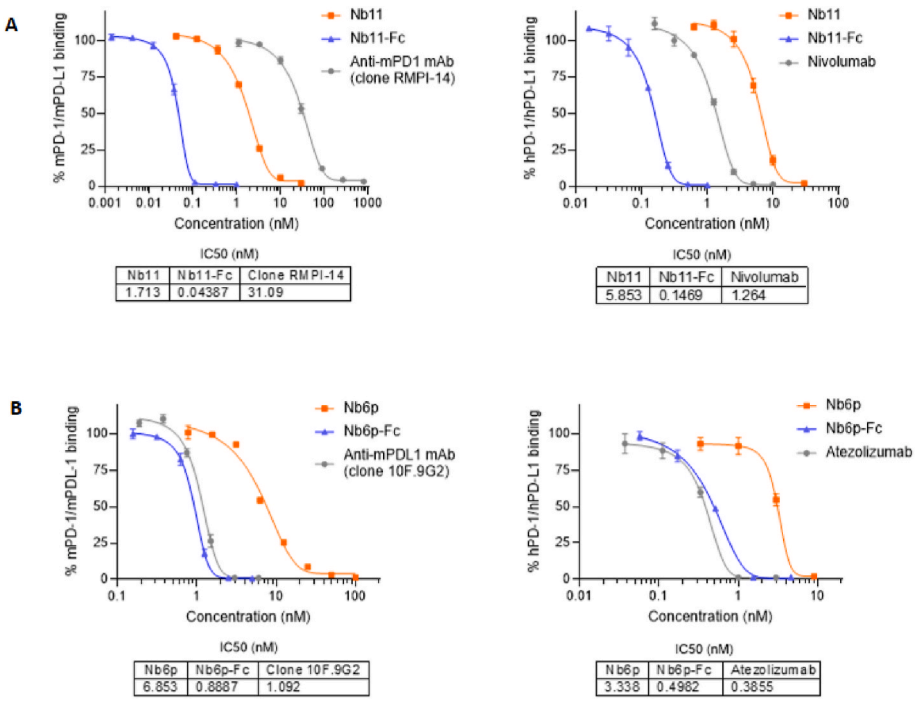

Fig. 3. Inhibition of PD-1/PD-L1 binding *in vitro*. Inhibition curves were performed using purified Nbs against PD-1 (**A**) and PD-L1 (**B**). Monomeric Nbs (orange), Nbs fused to Fc domains (blue), or commercially available antibodies (gray) were included in each assay. Mouse (left) or human (right) PD-1/PD-L1 ectodomains were used. Data represent mean ± SD of the percentage of PD-1/PD-L1 binding, considering the signal of wells with no blocking antibody as 100% of binding.

delaying tumor growth and significantly improving survival compared to control groups (saline and SFV-LacZ) (Fig. 4, left panels). Treatment with SFV-Nb11-Fc and SFV-Nb6p-Fc led to 53% and 60% long-term survival, respectively, in contrast to only 20% and 28% obtained with SFV-aPD1 and SFV-aPDL1, respectively (Fig. 4, middle panels). As observed before, monomeric Nbs showed a modest antitumor effect, which was similar or lower to that obtained with conventional antibodies. Treated animals that had complete remissions remained tumor-free after being rechallenged with MC38 cells (Fig. 4, right panels), suggesting that these treatments were able to generate an efficient memory immune response.

The efficacy of SFV-Nb11-Fc and SFV-Nb6p-Fc was also validated in melanoma tumor models (B16-OVA and B16–F10), where stabilization of disease and improvement in survival was observed in comparison with saline and SFV-LacZ groups, although no complete remissions were achieved in these models (Supplemental Figs. 2A and B). For B16 tumors, it has been described that a moderate liver damage is induced when they reach a certain size [34]. Serum transaminases were reduced in mice receiving SFV vectors indicating that our treatment can decrease liver damage (Supplemental Fig. 2C). In addition, amylase, which is a biomarker for pancreatic damage, was also significantly reduced in mice receiving SFV-Nb11-Fc. Although reduction in toxicity markers is likely a result of the antitumor effect induced by the SFV vector, it also indicates that no toxicity related to Nb expression was taking place. In fact, no significant differences in body weight were observed between mice receiving SFV vectors and saline, being control mice slightly heavier due to their larger tumor mass (Supplemental Fig. 2C).

One of the challenges for local immunotherapies is to trigger systemic antitumor effects. To evaluate whether SFV expressing dimeric Nbs could lead to abscopal effects in non-treated tumors, we used a bilateral subcutaneous MC38 tumor model. Mice received two intratumoral doses of SFV-Nb11-Fc vector (3×10^8 VPs/dose), five days apart, in one of the nodules. Although the vector led to a significant reduction in the size of the treated tumor, it had a more modest effect in terms of controlling the growth of non-treated nodules. A slight delay in growth from day nine onwards was observed in untreated tumors from mice that received SFV-Nb11-Fc compared to control mice that received saline, however, differences were not significant (Supplemental Figs. 3A and B). Nevertheless, treating only one tumor nodule with SFV-Nb11-Fc was enough to significantly increase the survival of mice compared to controls (Supplemental Fig. 3C).

3.5. *In vivo expression of Nbs from SFV vectors*

We then evaluated the levels and persistence of the different Nbs expressed from SFV administered locally in MC38 tumors using the same dose as in therapeutic experiments. We only observed expression of monomeric and Fc-fused Nbs in tumor tissue on day one post-treatment, while on day five Nb levels were undetectable in all mice (Fig. 5A). This is in line with previous observations using SFV vectors [11,35], and verifies the short-term expression attained by this non-propagative vector. In most cases Nbs were not detected in blood, but a significant leakage to systemic circulation was observed for Nb11-Fc on day one post-injection, with levels around 180 ng/mL (Fig. 5B). This might be due to the higher intratumoral expression obtained for this Nb compared to Nb6p-Fc, or to the fact that anti-PD-L1 Nbs could be retained more efficiently in the tumor microenvironment than anti-PD-1 Nbs due to the high PD-L1 expression in MC38 tumors [11]. We were also able to detect monomeric Nbs in urine, with a slight increase at day one, suggesting that these small molecules could be eliminated from circulation through renal clearance (Fig. 5C), while Nb11-Fc was detected at very low levels in urine at day one (Fig. 5D).

Although the immunogenicity of nanobodies is considered to be low [19], we evaluated the induction of anti-Nb11 antibodies in MC38-tumor bearing mice treated with two i.t. doses of SFV-Nb11-Fc (3×10^8 VPs/dose). Antibodies against Nb11 and SFV VP were measured by specific ELISAs fifteen days after the first dose. We observed induction of antibodies against Nb11 with a moderate titer (approx. 1350) in these animals (Supplemental Fig. 4A). As expected, the antibody titer against SFV were considerably higher (>12000). To test whether this immunogenicity could have been enhanced by the strategy of delivery, we administered Nb11 as recombinant purified protein in tumor-free

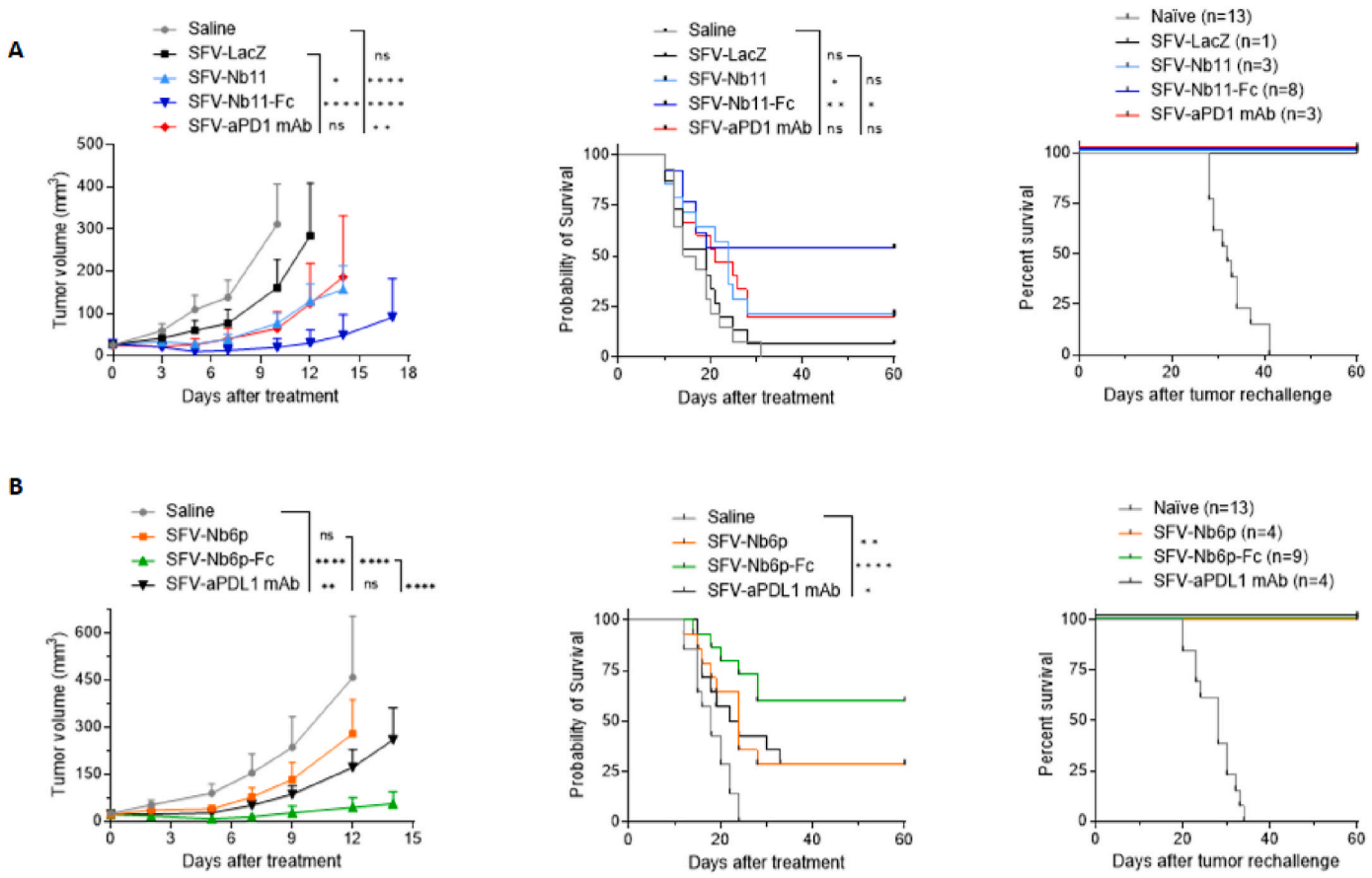

Fig. 4. Antitumor activity of SFV vectors encoding Nb-Fc fusion proteins. The antitumor activity of SFV vectors expressing Nbs or mAbs against PD-1 (**A**) and PD-L1 (**B**) was tested in the MC38 subcutaneous tumor model. When tumors reached a size of approximately 30 mm^3, a single intratumoral dose of 3×10^8 VPs of the indicated vectors was administered. SFV-LacZ and saline were used as controls. In A and B: left graphs, tumor growth evolution (mean ± SEM, a representative experiment out of two with similar results is shown, n = 6–8 per group); middle graphs, survival (pooled data from two independent experiments, n = 13–15 per group); right graphs, tumor growth evolution in cured mice rechallenged after 3 months with 5×10^5 MC38 cells in the left flank. Naïve untreated mice were included as controls. *, $p < 0.05$; **, $p < 0.01$; ****, $p < 0.0001$; ns, not significant.

mice, using three i.p. doses of 30 μg each, mimicking a standard treatment schedule. In this case, antibody titers against Nb11 measured fifteen days after the first dose were lower (approx. 150), suggesting that SFV could be playing a role in the development of anti-Nb11 antibodies (Supplemental Fig. 4B). Although anti-Nb11 antibodies may reduce the efficacy of subsequent doses of SFV-Nb11-Fc, the antitumor effect of a single dose showed to be very potent in the MC38 tumor model (Fig. 3).

3.6. Antitumor immune responses elicited by SFV encoding dimeric Nbs

To evaluate the antitumor immune responses elicited by SFV vectors encoding Nb-Fc fusion proteins, mice bearing MC38 tumors were treated with SFV-Nb11-Fc and SFV-Nb6p-Fc vectors, as well as with SFV-LacZ and saline as controls, and sacrificed five days later. Tumors and draining lymph nodes (dLNs) were processed and analyzed by flow-cytometry using different antibodies. In the case of SFV-Nb11-Fc, mice had very small tumors at the moment of sacrifice (with three complete remissions) and could not be included in this analysis (Fig. 6A). However, we did analyze changes in dLNs for both Nb groups.

A significant increase of total $CD8^+$ T cells was observed in tumors treated with SFV-Nb6p-Fc, which expressed higher levels of the activation marker ICOS and a trend to express higher levels of CD137 and granzyme B (Fig. 6B and Supplemental Figs. 5A–C). Although no relevant changes were observed in total MuLV tetramer-specific $CD8^+$ T cells in the SFV-Nb6p-Fc group, these cells showed a significant increase of the exhaustion marker TIM-3, suggesting a stronger activation state in this group (Fig. 6C and Supplemental Fig. 5D). No significant changes in PD-1 expression were observed in total and MuLV-specific $CD8^+$ T cells in tumors (Fig. 6D), as well as no global changes in the $CD4^+$ T cell population (data not shown). A higher percentage of NK cells ($NKp46^+$ cells) and myeloid cells ($CD11b^+$ cells) were found in tumors treated with SFV-Nb6p-Fc compared to saline and SFV-LacZ groups (Fig. 6E and Supplemental Figs. 5E and F). However, no changes were seen for macrophages ($F4/80^+CD11b^+$ cells), while there was a significant decrease in granulocytes ($Ly6G^+CD11b^+$ cells) (Fig. 6E).

In dLNs, although no global changes were observed for total $CD8^+$ T cells, this population showed significant lower levels of PD-1 and ICOS in mice treated with both SFV-Nb-Fc vectors, which might indicate a less activated phenotype in this location at the analyzed time point compared to controls (Supplemental Fig. 6A). In contrast to what was observed in tumors, $CD11b^+$ cells in dLNs showed a tendency to be decreased in response to both Nb-Fc treatments with no changes in PD-L1 expression (Supplemental Figs. 6B and C). A significant increase in $Ly6C^+CD11b^+$ cells was observed for SFV-Nb6p-Fc, and SFV-Nb11-Fc also showed a similar trend. Interestingly, these cells expressed lower levels of PD-L1 in both Nb-Fc groups (Supplemental Figs. 6B and C). Gating strategies are shown in Supplemental Fig. 7.

Tumor samples from animals treated with SFV-Nb11-Fc, SFV-LacZ or saline were used for bulk RNA sequencing analysis to gain a deeper insight into immune-related altered pathways. Several genes were found to be differentially expressed in tumors treated with SFV-Nb11-Fc compared to tumors injected with saline (Supplemental Fig. 8A). SFV-

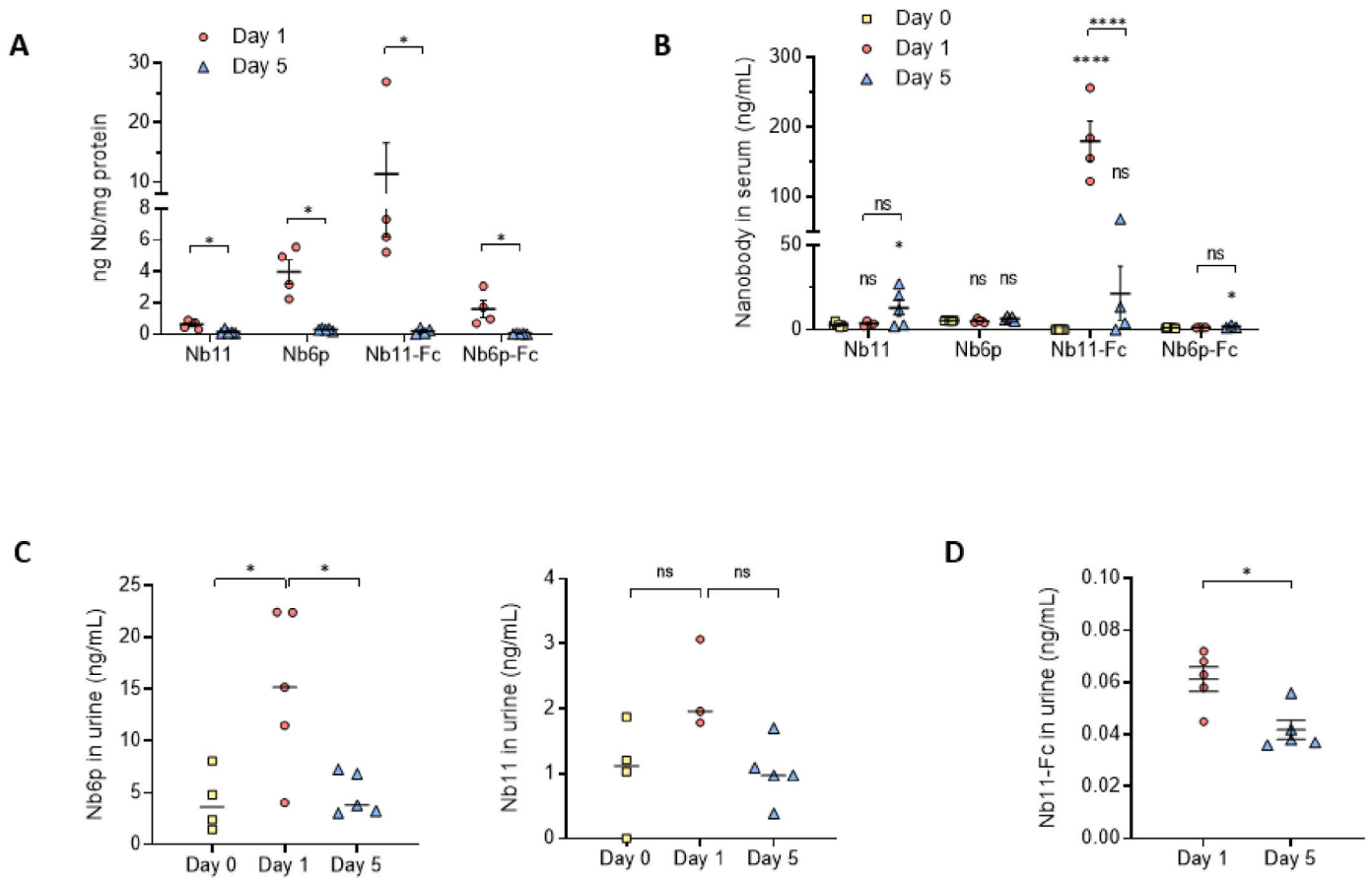

Fig. 5. Expression of Nbs *in vivo* from SFV vectors administered intratumorally. Mice bearing ~40 mm^3 subcutaneous MC38 tumors were injected intratumorally with 3×10^8 SFV VPs encoding monomeric or Fc-fused Nbs (n = 4–5 per group). Mice were sacrificed one or five days later to evaluate Nb expression *in vivo*. Nb levels in tumors (normalized by total protein content) (**A**) and in serum (**B**). Levels of monomeric Nb11 and Nb6p (**C**) and Nb11-Fc (**D**) in urine samples. *, $p < 0.05$; ****, $p < 0.0001$; ns, not significant.

LacZ vector was also able to induce important changes in the transcriptome in three out of five analyzed tumors, underlying the significance of SFV vector in immune modulation. However, changes were more homogenous and therefore more significant for tumors treated with SFV-Nb11-Fc. As expected, several viral-stress inducible genes (*Sting1*, *Batf2*, *Nod1*, *Tirap*, *Ikbke, Clec4d, Clec4e, Irf1*) were found upregulated in SFV-treated tumors. In addition, SFV-Nb11-Fc treatment generated an upregulation of different immunostimulatory genes, including cytokines (*Il2g*, *Il2ra*, *Il15ra*, *Il18rap*, *Ifng*, *Tgfa*), chemokines (*Cxcl9*, *Cxcl10*, *Cxcl11*), and IFN-I response genes (*Stat1*). The upregulation of molecules involved in cell adhesion and motility (such as *Icam1, Itgal*, *Selp*), suggests an increase in the recruitment of immune cell populations to the tumor site. Several genes associated with enhanced activity of NK cells and cytotoxic $CD8^+$ T cells (*Ncr1*, *Nkg7*, *Prf1, Gzma, Gzmb, Gzmk*), and genes expressed upon TCR stimulation (*Nfatc2*, *Lat*, *Cd6*, *Cd5*) were also upregulated, suggesting an increase in the infiltration and activation of these effector cells. Increased expression of genes related with apoptosis (*Cd40*, *Cd40lg*, *Fasl*, *Ripk1*) was also observed. Finally, SFV-Nb11-Fc treatment led to a downregulation of genes related with angiogenesis (*Vegfa* and *Jmjd8*), and pro-metastatic factors (*Cxcr4*, *Mmp11, Macc1*). The later are known markers of poor prognosis in different cancer types, including colorectal cancer [36–38].

Transcriptome differences between tumors treated with SFV-Nb11-Fc and SFV-LacZ were analyzed more extensively using the gene set enrichment analysis (GSEA) tool [39] and the C7 database, to compare changes in the immunologic signatures. Important differences were found for both treatment groups, and many of the altered gene sets were related to $CD8^+$ T cell activation, NK function, and IFN-γ signaling in different cells (Supplemental Fig. 8B).

In order to get a deeper insight into the immune responses mediated by SFV-Nb11-Fc, we also performed a side-by-side comparison of this therapy with systemic mAb administration, using a commercial anti-PD-1 antibody (clone RMPI-14). The antitumor effect was very similar for both treatments in the MC38 tumor model (Supplemental Fig. 9A). Fifteen days after the beginning of treatments, mice were sacrificed to characterize the tumor-infiltrating lymphocytes. We observed some differences between both groups, especially in the $CD8^+$ compartment. Animals treated with SFV-Nb11-Fc presented a trend to have higher numbers of $CD8^+$ T cells, and a significant increase in the number of tumor-specific T cells (measured by MuLV tetramer p15E) compared to untreated controls. Although a similar trend was observed in animals treated with anti-PD-1 mAb, no significant changes were achieved in this case compared to the saline group. We also observed a significant increase in effector $CD8^+$ T cells ($CD44^{high}$ $CD62L^-$) in animals treated with SFV compared to saline (Supplemental Fig. 9C). The percentage of $CD8^+$ T cells co-expressing PD-1, TIM-3 and LAG-3 was higher in animals that received anti-PD-1 mAb, which could indicate a more exhausted phenotype in these cells (Supplemental Figs. 9C and D). SFV-Nb11-Fc treatment seemed to induce downregulation of LAG-3 and upregulation of TIM-3 compared to saline and anti-PD-1 mAb (Supplemental Fig. 9D), suggesting a difference in the mechanism of action of both therapies.

3.7. Non-viral delivery of SFV vector encoding Nb11-Fc

The use of SFV VPs for clinical use has not been approved so far,

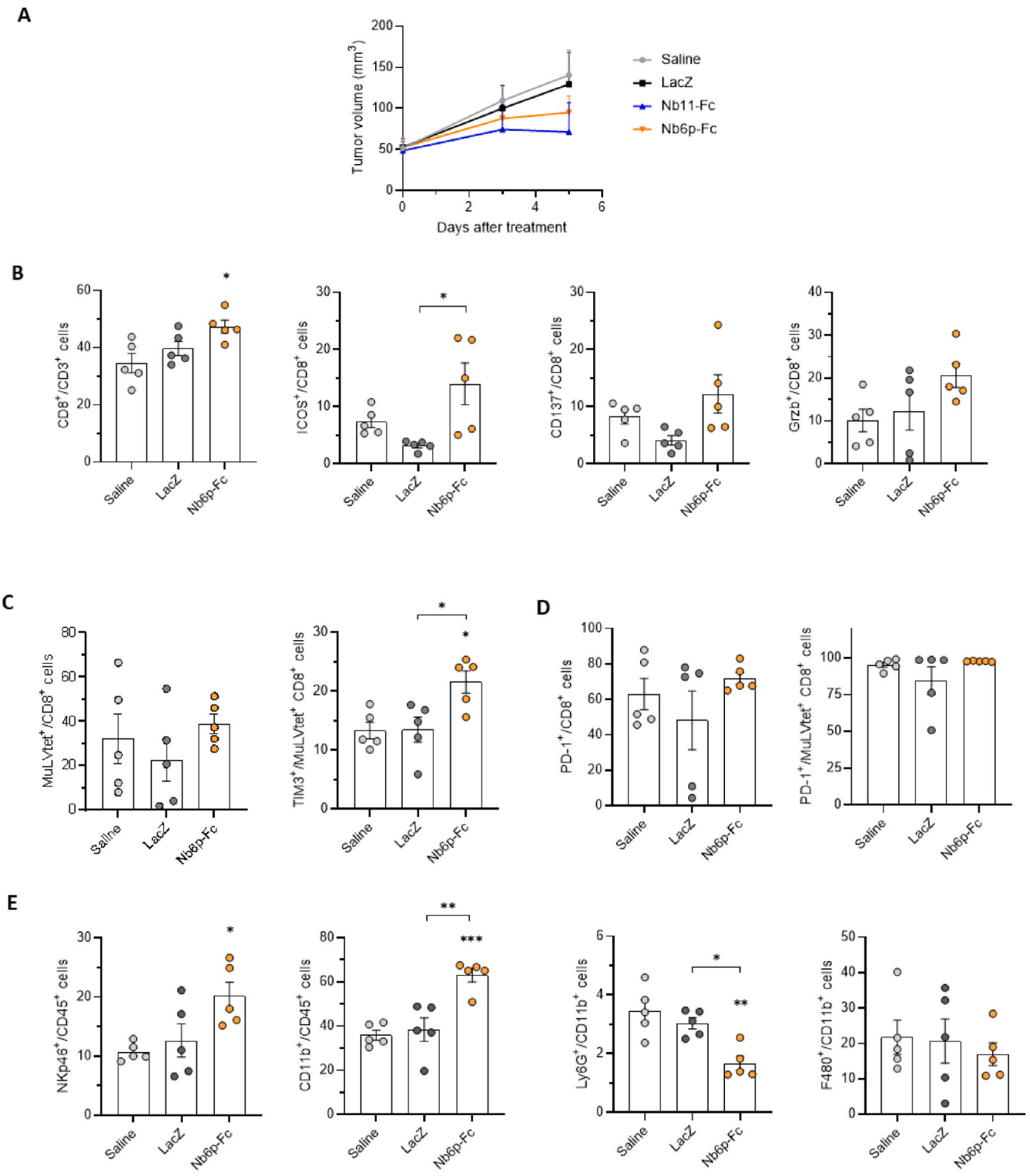

Fig. 6. Characterization of the immune cell infiltration in MC38 tumors treated with SFV vector encoding Nb6p-Fc. Mice bearing ~50 mm^3 MC38 tumors (n = 5–6/group) received one intratumoral dose of 3×10^8 SFV VPs, and five days later they were sacrificed to analyze the immune cell infiltrate by flow-cytometry. (**A**) Tumor growth curves until sacrifice. (**B**–**D**) Analysis of the $CD8^+$ T cell population in tumor samples. (**B**) $CD8^+$ T cell infiltration and expression of activation markers. (**C**) Analysis of MuLV-specific $CD8^+$ T cells. (**D**) PD-1 expression on $CD8^+$ T cells and MuLV-specific $CD8^+$ T cells. (**E**) Analysis of different innate immune cell populations in tumor samples. Asterisks above bars indicate comparisons to saline group. One sample from SFV-LacZ and one from SFV-Nb6p-Fc were excluded from this analysis due to low viability. *, $p < 0.05$; **, $p < 0.01$; ***, $p < 0.001$.

although a clinical trial has already been safely performed with this vector [40]. A possibility that could facilitate the clinical translatability of this strategy could be to use a non-viral approach to deliver SFV vectors into tumors. In fact, we have recently shown that SFV self-amplifying RNA can be delivered intratumorally by electroporation [28]. SFV can also be delivered as DNA using a plasmid in which the SFV vector sequence is placed under an eukaryotic promoter [41]. In this DNA/RNA layered system, the SFV RNA is transcribed in transfected cells, leading to high transgene expression levels and apoptosis in a similar way to SFV-infected cells. To test whether this delivery system could be used for SFV vectors expressing dimeric Nbs, we generated a plasmid containing the SFV-Nb11-Fc replicon under the transcriptional control of the CMV promoter (pBK-T-SFV-Nb11-Fc) (Fig. 7A). Expression of Nb11-Fc from this plasmid was confirmed *in vitro* by Western blot analysis of transfected BHK-21 cells (Fig. 7B). We also confirmed *in vivo* expression by electroporating pBK-T-SFV-Nb11-Fc into MC38 tumors, using SFV-Nb11-Fc VPs as control, and analyzing Nb11-Fc and SFV replicase expression by RT-qPCR at 24 h (Supplemental Fig. 10A). We observed very similar levels of both RNAs in DNA-electroporated and VP-infected tumors, suggesting that both methods of delivery could have a similar efficacy. Nb11-Fc levels detected in serum by ELISA were slightly higher in mice that received DNA electroporation, although differences were not significant (Supplemental Fig. 10B).

As schematized in Fig. 7C, mice bearing MC38 subcutaneous tumors received three doses of pBK-T-SFV-Nb11-Fc plasmid (20 μg/dose) every three days, followed by local electroporation as described previously by us [28]. This treatment protocol led to a significant reduction in tumor growth compared to untreated controls or mice that received SFV-LacZ plasmid by electroporation (Fig. 7D). A significant increase in survival for animals that received pBK-T-SFV-Nb11-Fc compared to untreated mice was also achieved (Fig. 7E). Similar to mice treated with viral vectors, this strategy led to 100% of protection after MC38 tumor rechallenge, suggesting that this non-viral delivery system is also able to promote long-lasting antitumor immune responses. The safety of DNA electroporation was confirmed in a similar experiment in which we observed that mice receiving pBK-T-SFV-Nb11 did not show hepatic or pancreatic toxicity, as indicated by the presence of normal transaminase and amylase levels, respectively (Supplemental Fig. 11A), or a decrease in body weight compared to control mice (Supplemental Fig. 11B). The therapeutic efficacy of pBK-T-SFV-Nb11-Fc was also confirmed in this study (Supplemental Fig. 11C).

4. Discussion

Antibodies able to block the PD-1/PD-L1 axis, such as nivolumab, pembrolizumab, and atezolizumab, are showing remarkable therapeutic effects in patients with different types of tumors [42]. However, frequent adverse effects observed in patients treated with ICIs, as well as the lack of responses in some tumor types, makes necessary the improvement of these therapies [43]. In this work, we have addressed these issues by developing a strategy based on local intratumoral delivery of Nbs using a self-amplifying RNA vector that can induce IFN-I responses and apoptosis in tumor cells, sensitizing tumors to ICIs [24].

The use of Nbs could offer some advantages over conventional antibodies, mainly due to their smaller size, which can allow these molecules to enter and be distributed more efficiently in tumors [20]. In addition, it has been described that Nbs can recognize conformational epitopes more efficiently than conventional antibodies due to their longer complementarity-determining region (CDR) 3 loop, which can form finger-like structures, allowing binding to small cavities or concave epitopes [44]. We have developed new Nbs against PD-L1 (Nb6p) and PD-1 (Nb11) [21] able to block the interactions of PD-1 and PD-L1 for both mouse and human molecules. The inhibition efficacy of Nb6p and Nb11 was improved by homo-dimerization using an IgG Fc domain, which resulted in a considerable IC50 reduction in PD-1/PD-L1 binding assays (approximately 8- and 40-fold reduction for Nb6p and Nb11, respectively, for both murine and human interactions). Remarkably, Nb11-Fc showed an IC50 that was 8.6-fold lower than nivolumab, and Nb6p-Fc had an IC50 very similar to atezolizumab. These results indicate that the newly described dimeric Nbs could have clinical potential as recombinant proteins, although they would need to be tested in humanized mouse models to evaluate their efficacy against human tumors. A similar anti-PD-L1 camel-derived Nb fused to a human IgG1 Fc, named envafolimab, has been recently approved for the treatment of various solid tumors in China, and it is being tested for soft tissue sarcomas and biliary tract cancer in the USA [45]. Interestingly, envafolimab is administered subcutaneously and has demonstrated a favorable safety profile. Envafolimab has shown an IC50 of 5.25 nM for blocking the PD-L1/PD-1 interaction [45], which is about 10-fold higher than the one we have observed for Nb6p-Fc, although a side by side study should be made to compare these two Nbs.

Despite the fact that dimeric Nbs are larger than their corresponding monomeric versions, their size is approximately half of conventional antibodies, which could endow them with a better penetrability in tumors, as it has been observed for envafolimab in animal models [46]. An additional advantage is the possibility to modulate the functions of Nbs using different Fc domains [47].

The improved blocking activity shown by dimeric Nbs *in vitro* was recapitulated *in vivo* when expressed from SFV vectors delivered intratumorally. Although SFV vectors encoding monomeric Nbs showed a modest antitumor activity in MC38 colon adenocarcinoma tumors, vectors encoding either Nb11-Fc or Nb6p-Fc had a potent antitumor effect in both colon and melanoma murine tumors, leading to more than 50% complete regressions in the first model. This effect was better than the one obtained with SFV vectors expressing anti-PD-L1 and anti-PD-1 conventional mAbs, although these vectors also showed significant antitumor effects, as previously described by us in the case of the SFV-aPDL1 [11]. One possible reason for the better performance of SFV vectors harboring dimeric Nbs could be the significantly higher expression levels of these molecules compared to mAbs, as it was observed *in vitro* in infected cells (Fig. 2C). *In vivo,* Nb expression was very transient with all vectors, being detected mainly one day after treatment. Although expression seemed to be restricted to tumors, in the case of Nb11-Fc a relatively high level was transiently observed in serum, suggesting that part of the dimeric Nb was able to leak out of the tumor. This effect was not observed for Nb6p-Fc, maybe due to the high expression of PD-L1 in MC38 tumors, previously reported by us and others [11,48], which might retain this Nb inside the tumor. Although in our study Nbs were expressed locally, it was also expected that for monomeric Nbs the fraction leaking out of the tumor would be eliminated rapidly through urine, as it seems to be the case since very low levels were detected in serum. Urine elimination of Nbs has been described as the main reason behind their short half-life *in vivo* [20]. Nb11-Fc was detected at higher levels in serum but at extremely low levels in urine, indicating that the Fc domain is preventing its elimination through renal clearance.

Despite being considered poorly immunogenic, antibodies against Nb11 were detected after administration of SFV-Nb11-Fc vector, which could decrease the efficacy of the treatment if subsequent doses are needed. However, the fact that circulating antibodies have low penetrability into tumors could mitigate this effect. In fact, we have previously shown that an SFV vector can efficiently reinfect tumors in the presence of high titers of circulating anti-SFV neutralizing antibodies [49]. Furthermore, in a previous study we were able to express Nb11 systemically in mice from an AAV vector during several months, which conferred protection against tumor challenge. This study suggested that, if they were present, anti-Nb11 antibodies were not able to completely block Nb11 activity [21]. In addition, strategies to decrease immunogenicity of nanobodies have been described [50,51] and could be tested in the future.

A remarkable feature of this SFV-based therapy is that a single dose of the vector expressing the dimerized Nb locally for a short period of

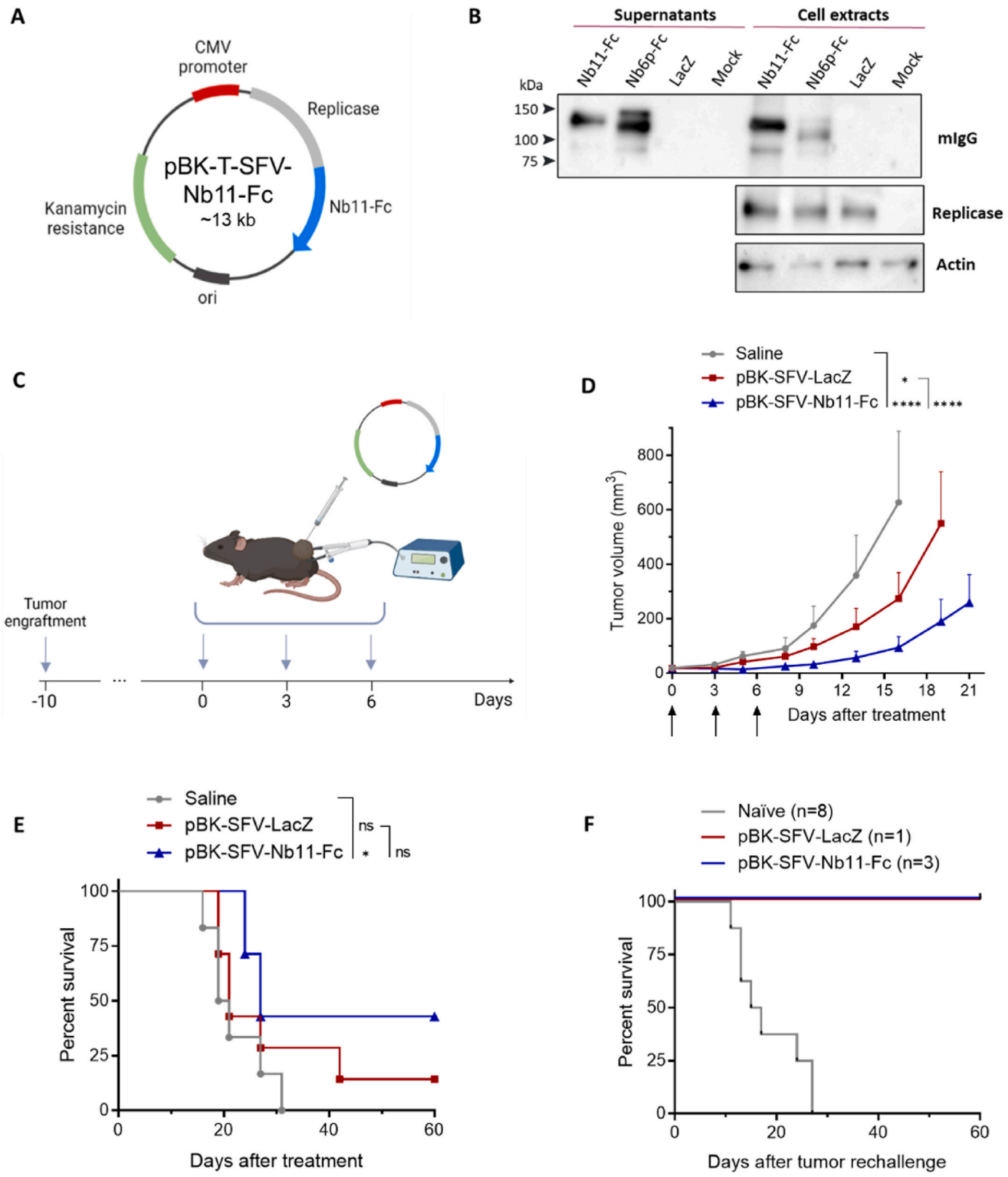

Fig. 7. Antitumor activity of a DNA/RNA layered SFV vector expressing Nb11-Fc delivered by local electroporation. (**A**) Schematic representation of pBK-T-SFV DNA plasmid vector harboring under the CMV promoter the SFV replicon encoding Nb11-Fc (pBK-SFV-Nb11-Fc). (**B**) Expression of Nb11-Fc from pBK-T-SFV-Nb11-Fc plasmid was confirmed *in vitro* by Western blot from transfected BHK-21 cells, including pBK-T-SFV-LacZ and pBK-T-SFV-Nb6p-Fc in this analysis. (**C**) Experimental design used for delivery of pBK-T-SFV plasmids into tumors. Mice bearing ~30 mm^3 MC38 subcutaneous tumors were injected intratumorally at the indicated times with 20 μg of SFV plasmids and electroporated as described in Materials & Methods. (**D**) Tumor growth curves. Data represent mean ± SEM (n = 6–7). Treatment days are indicated by arrows. (**E**) Survival curves for the treated animals. (**F**) Survival after MC38 tumor rechallenge in animals that had complete remissions after treatment. Naïve untreated mice were included as controls. *, $p < 0.05$; ****, $p < 0.0001$; ns, not significant.

time was able to promote potent and long-lasting antitumor responses. In fact, this antitumor effect was superior to the one induced by systemic and local administration of an anti-PD-L1 mAb, which was previously described by us in the same tumor model [11] and similar to the one obtained by systemic administration of an anti-PD-1 mAb (Supplemental Fig. 9). In previous studies we have shown that SFV vectors are able to induce type I IFN responses, which are very important to elicit efficient antitumor immune responses [11,52]. Here, we observed changes in different immune cell populations within tumors treated with SFV expressing Nb6p-Fc and Nb11-Fc, including NK and $CD8^+$ T cells, which are crucial effector cells in the antitumor response. As observed from RNAseq of total tumor samples, several immunostimulatory genes were significantly upregulated in tumors treated with SFV-Nb11-Fc compared to saline control group. In addition, the SFV control vector used in this study was also able to induce immunological changes within the tumor, highlighting the role of the self-amplifying RNA vector in this therapy. Despite this effect, the expression of dimerized Nbs able to block the PD-1/PD-L1 axis seemed to be crucial to trigger a curative immune response.

SFV viral particles can be produced quite efficiently [26] and a recent clinical trial in cervical cancer patients with SFV vectors expressing human papilloma (HPV) virus E6 and E7 proteins has demonstrated that they can be safely administered in humans [40]. However, clinical implementation of viral particles will be more difficult compared to the use of non-viral vectors, which are less expensive to produce at GMP levels and could have a higher safety profile. The SFV system has the advantage that it can also be used in a non-viral mode, either as RNA or as a DNA/RNA layered plasmid vector [41]. We have chosen this last option to evaluate one of the two SFV vectors expressing dimeric Nbs (pBK-T-SFV-Nb11-Fc). Interestingly, local delivery of this plasmid into MC38 tumors by electroporation resulted in antitumor effects comparable to those obtained with viral particles. *In vivo* electroporation of DNA has been evaluated in several clinical trials using a plasmid encoding IL-12 to treat melanoma, Merkel cell carcinoma, and triple-negative breast tumors, being able to induce tumor regressions [53–55]. Given the growing evidence that this technique is safe and able to provide antitumor effects, we believe that it could be a promising approach to deliver self-amplifying RNA vectors, either as RNA or DNA, as we have used in this work. An additional advantage of this strategy is that no neutralizing antibodies against SFV capsid will be induced, allowing for multiple administrations.

In summary, we believe that this short-term therapy based on the delivery of a self-amplifying RNA expressing dimeric Nbs to tumor cells, either as viral particles or DNA, could represent a promising new way to administer ICIs to cancer patients. The fact that both Nbs developed in this work are also able to block human PD-1/PD-L1 interactions makes these vectors potential new tools for clinical evaluation.

Financial support

This work was supported by the following grants: Instituto Salud Carlos III financed with Feder Funds PI20/00415 ("A way to make Europe"), Gobierno de Navarra. Departamento de Salud (GN2022/21), and PLEC2021-008094 funded by the Spanish Ministry of Science and Innovation MCIN/AEI/10.13039/501100011033 and European Union Next Generation EU/PRTR. NSP received a "Ayudas predoctorales de investigación biomédica AC" fellowship.

Author contributions

Conceptualization, supervision, project administration, and funding acquisition C.S. and L.V.; methodology, N.S–P. E.B., T.L., E.M., A.I., G. H–C., M.G., C.B–B. and P.S.; investigation, N.S–P., E.B. and L.V.; formal analysis, N.S–P., resources, C.S., L.V., G.G.S. and J.J.L; writing—original draft preparation, N.S–P. L.V. and C.S.; writing—review and editing, N. S–P., L.V., J.J.L. and C.S. All authors have read and agreed to the published version of the manuscript.

Declaration of competing interest

The authors declare the following financial interests/personal relationships which may be considered as potential competing interests: Lucía Vanrell declares being a co-founder of Nanogrow Biotech, a startup that develops nanobodies for pharmaceutical applications. The rest of the authors declare no conflict of interest.

Acknowledgements

We are grateful to personnel at the Cima Universidad de Navarra Animal Facility and at Parque Lecocq Uruguay for excellent assistance. We would like to thank personnel in the Genomic and Bioinformatics units at Cima Universidad de Navarra, especially Francesco Marchese and Elisabeth Guruceaga, for excellent help.

Appendix A. Supplementary data

Supplementary data to this article can be found online at https://doi.org/10.1016/j.canlet.2023.216139.

References

[1] K. Nakamura, M.J. Smyth, Myeloid immunosuppression and immune checkpoints in the tumor microenvironment, Cell. Mol. Immunol. 17 (2020) 1–12, https://doi.org/10.1038/s41423-019-0306-1.
[2] J.A. Seidel, A. Otsuka, K. Kabashima, Anti-PD-1 and anti-CTLA-4 therapies in cancer: mechanisms of action, efficacy, and limitations, Front. Oncol. 8 (2018) 86, https://doi.org/10.3389/fonc.2018.00086.
[3] P. Sharma, J.P. Allison, The future of immune checkpoint therapy, Science (80-.) 348 (2015) 56–61, https://doi.org/10.1126/science.aaa8172.
[4] Y. Yang, Cancer immunotherapy: harnessing the immune system to battle cancer, J. Clin. Invest. 125 (2015) 3335–3337, https://doi.org/10.1172/JCI83871.
[5] S. Bagchi, R. Yuan, E.G. Engleman, Immune checkpoint inhibitors for the treatment of cancer: clinical impact and mechanisms of response and resistance, Annu. Rev. Pathol. Mech. Dis. 16 (2021) 223–249, https://doi.org/10.1146/annurev-pathol-042020-042741.
[6] J.D. Twomey, B. Zhang, Cancer immunotherapy update: FDA-approved checkpoint inhibitors and companion diagnostics, AAPS J. 23 (2021) 39, https://doi.org/10.1208/s12248-021-00574-0.
[7] N. Abdel-Wahab, M. Shah, M.E. Suarez-Almazor, Adverse events associated with immune checkpoint blockade in patients with cancer: a systematic review of case reports, PLoS One 11 (2016), e0160221, https://doi.org/10.1371/journal.pone.0160221.
[8] J.W. Hommes, R.J. Verheijden, K.P.M. Suijkerbuijk, D. Hamann, Biomarkers of checkpoint inhibitor induced immune-related adverse events—a comprehensive review, Front. Oncol. 10 (2021), https://doi.org/10.3389/fonc.2020.585311.
[9] S. Das, D.B. Johnson, Immune-related adverse events and anti-tumor efficacy of immune checkpoint inhibitors, J. Immunother. Cancer 7 (2019) 306, https://doi.org/10.1186/s40425-019-0805-8.
[10] M.A. Aznar, N. Tinari, A.J. Rullán, A.R. Sánchez-Paulete, M.E. Rodriguez-Ruiz, I. Melero, Intratumoral delivery of immunotherapy-act locally, think globally, J. Immunol. 198 (2017) 31–39, https://doi.org/10.4049/jimmunol.1601145.
[11] M.C. Ballesteros-Briones, E. Martisova, E. Casales, N. Silva-Pilipich, M. Buñuales, J. Galindo, U. Mancheño, M. Gorraiz, J.J. Lasarte, G. Kochan, D. Escors, A. R. Sanchez-Paulete, I. Melero, J. Prieto, R. Hernandez-Alcoceba, S. Hervas-Stubbs, C. Smerdou, Short-term local expression of a PD-L1 blocking antibody from a self-replicating RNA vector induces potent antitumor responses, Mol. Ther. 27 (2019) 1892–1905, https://doi.org/10.1016/j.ymthe.2019.09.016.
[12] C.E. Engeland, C. Grossardt, R. Veinalde, S. Bossow, D. Lutz, J.K. Kaufmann, I. Shevchenko, V. Umansky, D.M. Nettelbeck, W. Weichert, D. Jäger, C. von Kalle, G. Ungerechts, CTLA-4 and PD-L1 checkpoint blockade enhances oncolytic measles virus therapy, Mol. Ther. 22 (2014), https://doi.org/10.1038/mt.2014.160, 1949–59.
[13] L. Milling, Y. Zhang, D.J. Irvine, Delivering safer immunotherapies for cancer, Adv. Drug Deliv. Rev. 114 (2017) 79–101, https://doi.org/10.1016/j.addr.2017.05.011.
[14] S.N. Smith, R. Schubert, B. Simic, D. Brücher, M. Schmid, N. Kirk, P.C. Freitag, V. Gradinaru, A. Plückthun, The SHREAD gene therapy platform for paracrine delivery improves tumor localization and intratumoral effects of a clinical antibody, Proc. Natl. Acad. Sci. USA 118 (2021), https://doi.org/10.1073/pnas.2017925118.
[15] C. Hamers-Casterman, T. Atarhouch, S. Muyldermans, G. Robinson, C. Hammers, E.B. Songa, N. Bendahman, R. Hammers, Naturally occurring antibodies devoid of light chains, Nature 363 (1993) 446–448, https://doi.org/10.1038/363446a0.
[16] C. Sheridan, Ablynx's nanobody fragments go places antibodies cannot, Nat. Biotechnol. 35 (2017) 1115–1117, https://doi.org/10.1038/nbt1217-1115.

[17] A. de Marco, Recombinant expression of nanobodies and nanobody-derived immunoreagents, Protein Expr. Purif. 172 (2020), 105645, https://doi.org/10.1016/J.PEP.2020.105645.

[18] M.E. Iezzi, L. Policastro, S. Werbajh, O. Podhajcer, G.A. Canziani, Single-domain antibodies and the promise of modular targeting in cancer imaging and treatment, Front. Immunol. 9 (2018), https://doi.org/10.3389/fimmu.2018.00273.

[19] C. Ackaert, N. Smiejkowska, C. Xavier, Y.G.J. Sterckx, S. Denies, B. Stijlemans, Y. Elkrim, N. Devoogdt, V. Caveliers, T. Lahoutte, S. Muyldermans, K. Breckpot, M. Keyaerts, Immunogenicity risk profile of nanobodies, Front. Immunol. 12 (2021), https://doi.org/10.3389/fimmu.2021.632687.

[20] M. Kijanka, B. Dorresteijn, S. Oliveira, P.M. van Bergen en Henegouwen, Nanobody-based cancer therapy of solid tumors, Nanomedicine 10 (2015) 161–174, https://doi.org/10.2217/nnm.14.178.

[21] N. Silva-Pilipich, E. Martisova, M.C. Ballesteros-Briones, S. Hervas-Stubbs, N. Casares, G. González-Sapienza, C. Smerdou, L. Vanrell, Long-term systemic expression of a novel PD-1 blocking nanobody from an AAV vector provides antitumor activity without toxicity, Biomedicines 8 (2020), https://doi.org/10.3390/biomedicines8120562.

[22] J.I. Quetglas, S. Labiano, M.Á. Aznar, E. Bolaños, A. Azpilikueta, I. Rodriguez, E. Casales, A.R. Sánchez-Paulete, V. Segura, C. Smerdou, I. Melero, Virotherapy with a semliki forest virus–based vector encoding IL12 synergizes with PD-1/PD-L1 blockade, cancer immunol, Res. 3 (2015) 449–454, https://doi.org/10.1158/2326-6066.CIR-14-0216.

[23] J.I. Quetglas, J. Fioravanti, N. Ardaiz, J. Medina-Echeverz, I. Baraibar, J. Prieto, C. Smerdou, P. Berraondo, A Semliki Forest virus vector engineered to express IFNα induces efficient elimination of established tumors, Gene Ther. 19 (2012) 271–278, https://doi.org/10.1038/gt.2011.99.

[24] J.I. Quetglas, M. Ruiz-Guillen, A. Aranda, E. Casales, J. Bezunartea, C. Smerdou, Alphavirus vectors for cancer therapy, Virus Res. 153 (2010) 179–196, https://doi.org/10.1016/j.virusres.2010.07.027.

[25] P. Liljeström, H. Garoff, Expression of proteins using Semliki Forest virus vectors, Curr. Protoc. Mol. Biol. (2001), https://doi.org/10.1002/0471142727.mb1620s29.

[26] C. Smerdou, P. Liljeström, Two-helper RNA system for production of recombinant semliki forest virus particles, J. Virol. 73 (1999) 1092–1098, https://doi.org/10.1128/JVI.73.2.1092-1098.1999.

[27] M.N. Fleeton, B.J. Sheahan, E.A. Gould, G.J. Atkins, P. Liljestr√∂m, Recombinant Semliki Forest virus particles encoding the prME or NS1 proteins of louping ill virus protect mice from lethal challenge, J. Gen. Virol. 80 (1999) 1189–1198, https://doi.org/10.1099/0022-1317-80-5-1189.

[28] N. Silva-Pilipich, A. Lasarte-Cía, T. Lozano, C. Martín-Otal, J.J. Lasarte, C. Smerdou, Intratumoral electroporation of a self-amplifying RNA expressing IL-12 induces antitumor effects in mouse models of cancer, Mol. Ther. Nucleic Acids 29 (2022) 387–399, https://doi.org/10.1016/j.omtn.2022.07.020.

[29] N. Silva-Pilipich, C. Smerdou, L. Vanrell, A small virus to deliver small antibodies: new targeted therapies based on AAV delivery of nanobodies, Microorganisms 9 (2021) 1956, https://doi.org/10.3390/microorganisms9091956.

[30] Godakova, Vinogradova Noskov, Solovyev Ugriumova, Tukhvatulin Esmagambetov, Naroditsky Logunov, Shcheblyakov, Gintsburg, Camelid VHHs fused to human Fc fragments provide long term protection against botulinum neurotoxin A in mice, Toxins (Basel). 11 (2019) 464, https://doi.org/10.3390/toxins11080464.

[31] C. Sun, R. Mezzadra, T.N. Schumacher, Regulation and function of the PD-L1 checkpoint, Immunity 48 (2018) 434–452, https://doi.org/10.1016/j.immuni.2018.03.014.

[32] C. Grasselly, M. Denis, A. Bourguignon, N. Talhi, D. Mathe, A. Tourette, L. Serre, L. P. Jordheim, E.L. Matera, C. Dumontet, The antitumor activity of combinations of cytotoxic chemotherapy and immune checkpoint inhibitors is model-dependent, Front. Immunol. 9 (2018), https://doi.org/10.3389/fimmu.2018.02100.

[33] S.F. Ngiow, A. Young, N. Jacquelot, T. Yamazaki, D. Enot, L. Zitvogel, M.J. Smyth, A threshold level of intratumor CD8+ T-cell PD1 expression dictates therapeutic response to anti-PD1, Cancer Res. 75 (2015) 3800–3811, https://doi.org/10.1158/0008-5472.CAN-15-1082.

[34] T. Eggert, J. Medina-Echeverz, T. Kapanadze, M.J. Kruhlak, F. Korangy, T. F. Greten, Tumor induced hepatic myeloid derived suppressor cells can cause moderate liver damage, PLoS One 9 (2014), e112717, https://doi.org/10.1371/journal.pone.0112717.

[35] J.R. Rodriguez-Madoz, J. Prieto, C. Smerdou, Semliki forest virus vectors engineered to express higher IL-12 levels induce efficient elimination of murine colon adenocarcinomas, Mol. Ther. 12 (2005) 153–163, https://doi.org/10.1016/j.ymthe.2005.02.011.

[36] U. Stein, MACC1 – a novel target for solid cancers, Expert Opin. Ther. Targets 17 (2013) 1039–1052, https://doi.org/10.1517/14728222.2013.815727.

[37] S. Chatterjee, B. Behnam Azad, S. Nimmagadda, The intricate role of CXCR4 in cancer, Adv. Cancer Res. (2014) 31–82, https://doi.org/10.1016/B978-0-12-411638-2.00002-1.

[38] B. Ma, R. Ran, H.-Y. Liao, H.-H. Zhang, The paradoxical role of matrix metalloproteinase-11 in cancer, Biomed. Pharmacother. 141 (2021), 111899, https://doi.org/10.1016/j.biopha.2021.111899.

[39] A. Subramanian, P. Tamayo, V.K. Mootha, S. Mukherjee, B.L. Ebert, M.A. Gillette, A. Paulovich, S.L. Pomeroy, T.R. Golub, E.S. Lander, J.P. Mesirov, Gene set enrichment analysis: a knowledge-based approach for interpreting genome-wide expression profiles, Proc. Natl. Acad. Sci. USA 102 (2005) 15545–15550, https://doi.org/10.1073/pnas.0506580102.

[40] F.L. Komdeur, A. Singh, S. van de Wall, J.J.M. Meulenberg, A. Boerma, B. N. Hoogeboom, S.T. Paijens, C. Oyarce, M. de Bruyn, E. Schuuring, J. Regts, R. Marra, N. Werner, J. Sluis, A.G.J. van der Zee, J.C. Wilschut, D.P. Allersma, C. J. van Zanten, J.G.W. Kosterink, A. Jorritsma-Smit, R. Yigit, H.W. Nijman, T. Daemen, First-in-Human phase I clinical trial of an SFV-based RNA replicon cancer vaccine against HPV-induced cancers, Mol. Ther. 29 (2021) 611–625, https://doi.org/10.1016/j.ymthe.2020.11.002.

[41] C. Smerdou, P. Liljeström, Non-viral amplification systems for gene transfer: vectors based on alphaviruses, Curr. Opin. Mol. Therapeut. 1 (1999) 244–251.

[42] Z. Xiang, J. Li, Z. Zhang, C. Cen, W. Chen, B. Jiang, Y. Meng, Y. Wang, B. Berglund, G. Zhai, J. Wu, Comprehensive evaluation of anti-PD-1, anti-PD-L1, anti-CTLA-4 and their combined immunotherapy in clinical trials: a systematic review and meta-analysis, Front. Pharmacol. 13 (2022), 883655, https://doi.org/10.3389/fphar.2022.883655.

[43] G. Sun, H. Liu, X. Shi, P. Tan, W. Tang, X. Chen, G. Sun, W. Yang, X. Kong, Z. Zheng, H. Cao, G. Shao, Treatment of patients with cancer using PD-1/PD-L1 antibodies: adverse effects and management strategies (Review), Int. J. Oncol 60 (74) (2022), https://doi.org/10.3892/ijo.2022.5364.

[44] I. Jovčevska, S. Muyldermans, The therapeutic potential of nanobodies, BioDrugs 34 (2020) 11–26, https://doi.org/10.1007/s40259-019-00392-z.

[45] A. Markham, Envafolimab: first approval, Drugs 82 (2022) 235–240, https://doi.org/10.1007/s40265-022-01671-w.

[46] A. Akinleye, Z. Rasool, Immune checkpoint inhibitors of PD-L1 as cancer therapeutics, J. Hematol. Oncol. 12 (2019) 92, https://doi.org/10.1186/s13045-019-0779-5.

[47] A.I. Schriek, M.M. van Haaren, M. Poniman, G. Dekkers, A.E.H. Bentlage, M. Grobben, G. Vidarsson, R.W. Sanders, T. Verrips, T.B.H. Geijtenbeek, R. Heukers, N.A. Kootstra, S.W. de Taeye, M.J. van Gils, Anti-HIV-1 nanobody-IgG1 constructs with improved neutralization potency and the ability to mediate Fc effector functions, Front. Immunol. 13 (2022), 893648, https://doi.org/10.3389/fimmu.2022.893648.

[48] J.W. Kleinovink, K.A. Marijt, M.J.A. Schoonderwoerd, T. van Hall, F. Ossendorp, M.F. Fransen, PD-L1 expression on malignant cells is no prerequisite for checkpoint therapy., OncoImmunology. 6 (n.d.) e1294299. https://doi.org/10.1080/2162402X.2017.1294299..

[49] J.R. Rodriguez-Madoz, J. Prieto, C. Smerdou, Biodistribution and tumor infectivity of semliki forest virus vectors in mice: effects of re-administration, Mol. Ther. 15 (2007) 2164–2171, https://doi.org/10.1038/sj.mt.6300274.

[50] C. Vincke, R. Loris, D. Saerens, S. Martinez-Rodriguez, S. Muyldermans, K. Conrath, General strategy to humanize a camelid single-domain antibody and identification of a universal humanized nanobody scaffold, J. Biol. Chem. 284 (2009) 3273–3284, https://doi.org/10.1074/jbc.M806889200.

[51] Z. Sang, Y. Xiang, I. Bahar, Y. Shi, Llamanade: an open-source computational pipeline for robust nanobody humanization, Structure 30 (2022) 418–429, https://doi.org/10.1016/j.str.2021.11.006, e3.

[52] I. Melero, J.I. Quetglas, M. Reboredo, J. Dubrot, J.R. Rodriguez-Madoz, U. Mancheño, E. Casales, J.I. Riezu-Boj, M. Ruiz-Guillen, M.C. Ochoa, M. F. Sanmamed, N. Thieblemont, C. Smerdou, S. Hervas-Stubbs, Strict requirement for vector-induced type I interferon in efficacious antitumor responses to virally encoded IL12, Cancer Res. 75 (2015) 497–507, https://doi.org/10.1158/0008-5472.CAN-13-3356.

[53] S.K. Greaney, A.P. Algazi, K.K. Tsai, K.T. Takamura, L. Chen, C.G. Twitty, L. Zhang, A. Paciorek, R.H. Pierce, M.H. Le, A.I. Daud, L. Fong, Intratumoral plasmid IL12 electroporation therapy in patients with advanced melanoma induces systemic and intratumoral T-cell responses, Cancer Immunol. Res. 8 (2020) 246–254, https://doi.org/10.1158/2326-6066.CIR-19-0359.

[54] S. Bhatia, N.V. Longino, N.J. Miller, R. Kulikauskas, J.G. Iyer, D. Ibrani, A. Blom, D. R. Byrd, U. Parvathaneni, C.G. Twitty, J.S. Campbell, M.H. Le, S. Gargosky, R. H. Pierce, R. Heller, A.I. Daud, P. Nghiem, Intratumoral delivery of plasmid IL12 via electroporation leads to regression of injected and noninjected tumors in Merkel cell carcinoma, Clin. Cancer Res. 26 (2020) 598–607, https://doi.org/10.1158/1078-0432.CCR-19-0972.

[55] M.L. Telli, H. Nagata, I. Wapnir, C.R. Acharya, K. Zablotsky, B.A. Fox, C.B. Bifulco, S.M. Jensen, C. Ballesteros-Merino, M.H. Le, R.H. Pierce, E. Browning, R. Hermiz, L. Svenson, D. Bannavong, K. Jaffe, J. Sell, K.M. Foerter, D.A. Canton, C.G. Twitty, T. Osada, H.K. Lyerly, E.J. Crosby, Intratumoral plasmid IL12 expands CD8+ T cells and induces a CXCR3 gene signature in triple-negative breast tumors that sensitizes patients to anti–PD-1 therapy, Clin. Cancer Res. 27 (2021) 2481–2493, https://doi.org/10.1158/1078-0432.CCR-20-3944.